

Variational Calculation of Highly Excited Rovibrational Energy Levels of H₂O₂

Oleg L. Polyansky,^{†,‡} Igor N. Kozin,[‡] Roman I. Ovsyannikov,[‡] Paweł Małyszek,[§] Jacek Koput,[§] Jonathan Tennyson,^{*,†} and Sergei N. Yurchenko[†]

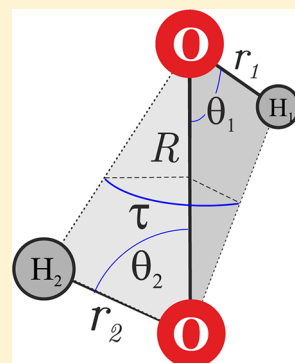
[†]Department of Physics and Astronomy, University College London, London WC1E 6BT, United Kingdom

[‡]Institute of Applied Physics, Russian Academy of Science, Ulyanov Street 46, Nizhny Novgorod, Russia 603950

[§]Department of Chemistry, Adam Mickiewicz University, Poznan, Poland

Supporting Information

ABSTRACT: Results are presented for highly accurate ab initio variational calculation of the rotation–vibration energy levels of H₂O₂ in its electronic ground state. These results use a recently computed potential energy surface and the variational nuclear–motion programs WARV4, which uses an exact kinetic energy operator, and TROVE, which uses a numerical expansion for the kinetic energy. The TROVE calculations are performed for levels with high values of rotational excitation, J up to 35. The purely ab initio calculations of the rovibrational energy levels reproduce the observed levels with a standard deviation of about 1 cm^{−1}, similar to that of the $J = 0$ calculation, because the discrepancy between theory and experiment for rotational energies within a given vibrational state is substantially determined by the error in the vibrational band origin. Minor adjustments are made to the ab initio equilibrium geometry and to the height of the torsional barrier. Using these and correcting the band origins using the error in $J = 0$ states lowers the standard deviation of the observed–calculated energies to only 0.002 cm^{−1} for levels up to $J = 10$ and 0.02 cm^{−1} for all experimentally known energy levels, which extend up to $J = 35$.



INTRODUCTION

Hydrogen peroxide (H₂O₂) is a well-studied system because of its unusual properties, particularly the almost freely rotating OH moieties. The role of H₂O₂ in the chemistry of the Earth's atmosphere^{1–3} as well as of the Martian atmosphere^{4,5} has been widely acknowledged. It has also recently been detected in the interstellar medium.⁶ The vibration–rotation spectra of hydrogen peroxide has attracted significant attention, both experimental and theoretical. For example, it has been used as a benchmark system with large amplitude motion for testing different variational nuclear motion codes.^{7–15}

Very recently, Małyszek and Koput¹⁶ presented a highly accurate ab initio potential energy surface (PES) of HOOH, which was shown to reproduce the known vibrational band origins with an average accuracy of 1 cm^{−1}. Other ab initio PESs of HOOH were reported by Harding,¹⁷ Kuhn et al.,¹⁸ Senent et al.,¹⁹ and Koput et al.²⁰

Hydrogen peroxide has three important properties from the viewpoint of variational calculations: first, the large amplitude motion of the OH internal rotors that has already been mentioned; second, its relatively low dissociation energy of ~17 000 cm^{−1} has made H₂O₂ a benchmark tetratomic molecule for experimental study of the dissociation process;²¹ and third, H₂O₂ is a tetratomic system for which variational calculations can really aid the analysis of spectra.

For triatomic molecules, accurate calculation of the rotation–vibration levels to high accuracy using variational nuclear

motion methods has become routine.^{22–24} For tetratomic molecules, this process is just beginning; it is natural for initial high-accuracy studies to focus on molecules with large amplitude motions, such as ammonia^{25,26} and hydrogen peroxide.

The advantages of using variational calculations to assign vibration–rotation spectra of triatomic molecules has been demonstrated for several molecules. Initial studies focused on H₃⁺^{27–29} and water,^{30,31} systems for which the use of variational calculations to analyze spectra is now the accepted procedure. In particular, spectra involving hot molecules and, hence, high rotational states and large amplitude motion, such as H₃⁺ on Jupiter²⁷ and water on the Sun,³⁰ assignments using the traditional, effective Hamiltonian approach are almost impossible.

A significant advantage of variational calculations over effective Hamiltonian techniques is the automatic allowance for accidental resonances between vibrations. Whereas for most triatomic molecules such resonances become significant at fairly high vibrational energies, for tetratomic molecules, accidental resonances can even make the analysis of low-lying vibrational states intractable using effective Hamiltonians. H₂O₂ is a good

Special Issue: Joel M. Bowman Festschrift

Received: February 2, 2013

Revised: April 17, 2013

example of this situation. Although H_2O_2 spectral lines are strong and were first observed more than 70 years ago with spectrometers much less sophisticated than those available nowadays,^{32,33} the analysis of experimental spectra involving high J transitions for H_2O_2 is complete only up to 2000 cm^{-1} ,^{34–36} significantly lower in frequency than transitions to the OH stretching fundamentals. One reason for this is the complication of the analysis by accidental resonances. Accurate variational calculations on H_2O_2 offer a way out of this impasse.

Recent advances in variational calculations suggest that they can be used for systems larger than triatomic. High-accuracy variational calculations of the spectra and line lists for tetratomic molecules such as ammonia^{26,37,38} have been performed. These NH_3 line lists have been used both for the assignment of transitions involving higher vibrational states³⁹ and hot rovibrational spectra involving high J levels⁴⁰ and for correcting and improving the analysis of more standard transitions.^{26,41} Numerical calculations of wave functions for high- J states of tetratomic molecules are possible not only because modern computers have the ability to diagonalize larger matrices but also because, as illustrated below, the accuracy of calculations employing approximate kinetic energy operators^{42,43} becomes comparable with those using an exact kinetic energy approach.⁴⁴ Although high- J calculations within the exact kinetic energy approach are still computationally challenging for tetratomic molecules, calculations with $J \sim 50$ are feasible with approaches such as TROVE.⁴³ Furthermore, the possibility of calculating ab initio dipole moment surfaces of extremely high accuracy⁴⁵ enhances the value of using variational calculations because they can also be used to create line lists. These factors raise the possibility of creating accurate line lists for H_2O_2 ; however, the presence of the large-amplitude, torsional motion of the two OH fragments in H_2O_2 complicates the problem. This requires an appropriate nuclear motion program for calculation of the rovibrational energy levels by solving the corresponding Schrödinger equation; this program should be able to compute high J levels within the limitations of the modern computers.

In this paper, we compute high-accuracy rovibrational energy levels going to high J for H_2O_2 using the ab initio PES due to Malyszczek and Koput.¹⁶ To do this, we test two nuclear motion programs: the exact kinetic energy (EKE) program WAVR4⁴⁶ and approximate kinetic energy program TROVE.⁴³ It is shown that use of TROVE allows us to calculate very high J energy levels, which are in excellent agreement with observation. The paper is organized as follows. Section 2 describes the modifications of the TROVE program necessary to make it suitable for the calculation of spectra of such a nonrigid molecule. Section 3 describes the details of computations performed. Section 4 presents our results and is followed by the concluding section, which discusses prospects for further work on this system.

METHODS OF CALCULATION

The accuracy of a calculation of rovibrational energy levels depends first of all on the accuracy of the potential energy surface (PES) used as input to the nuclear motion Schrödinger equation. Until recently, the most accurate PES for H_2O_2 was the one due to Koput et al.,²⁰ which gave a typical discrepancy between theory and experiment for vibrational band origins of $\sim 10 \text{ cm}^{-1}$.⁴⁷ However, two of us¹⁶ recently determined a very accurate PES computed using the explicitly correlated coupled-cluster method [CCSD(T)-F12] method,^{48,49} in the F12b

form,⁵⁰ as implemented in the MOLPRO package.⁵¹ Various correlation-consistent basis sets were used for various parts of the PES, the largest being aug-cc-pV7Z. The CCSD(T)-F12 results were augmented with the Born–Oppenheimer diagonal, higher-order valence-electron correlation, relativistic, and core–electron correlation corrections. The 1762 ab initio points obtained were fitted to the functional form

$$V(q_1, q_2, q_3, q_4, q_5, q_6) = \sum_{ijklmn} c_{ijklmn} q_1^i q_2^j q_3^k q_4^l q_5^m \cos nq_6 \quad (1)$$

where q_i ($i = 1, 2, 3$) are the Simons–Parr–Finlan stretching OO and OH coordinates⁵² $q_3 = (R - R_e)/R$ and $q_i = (r_i - r_e)/r$ ($i = 1, 2$); $q_4 = \theta_1 - \theta_e$ and $q_5 = \theta_2 - \theta_e$ are the two OOH bending coordinates; $q_6 = \tau$ is the torsional angle $\angle\text{HOOH}$ (see Figure 1); and R_e , r_e , and θ_e are the corresponding equilibrium values. The expansion coefficients c_{ijklmn} used in this work are given in the Supporting Information (see also ref 16.).

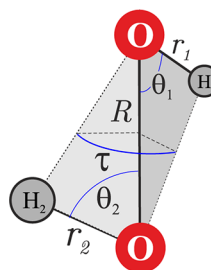


Figure 1. The internal coordinates for the HOOH molecule.

Recent calculations¹⁶ using this PES gave, for the 30 observed vibrational band origins of H_2O_2 , a standard deviation for the observed minus calculated (obs – calc) wavenumbers of about 1 cm^{-1} , an order of magnitude improvement over the previous results.⁴⁷ An ab initio line list with this accuracy could be useful for a number of applications; however, for most applications, it is also necessary to accurately compute highly excited rotational levels. This is done in this work. Before looking at high- J rotational levels, we reconsidered the $J = 0$ results of Malyszczek and Koput¹⁶ using both the EKE program WAVR4⁴⁶ and the approximate kinetic energy program TROVE.⁴³

Diatom–diatom HO–OH coordinates were employed in the program WAVR4; these coordinates were one of those used to consider acetylene–vinylidene isomerization.⁵³ The calculations used a discrete variable representation (DVR)⁵⁴ based on a grid of 10 radial functions for each OH coordinate and 18 radial functions for the OO coordinate. The parameters used for OH stretch Morse-oscillator-like functions were $R_e = 0.91 \text{ \AA}$, $\omega_e = 2500 \text{ cm}^{-1}$, and $D_e = 35\,000 \text{ cm}^{-1}$; and $r_e = 1.53 \text{ \AA}$, $\omega_e = 1500 \text{ cm}^{-1}$, and $D_e = 45\,000 \text{ cm}^{-1}$ for the OO stretch. The bending basis set consists of coupled angular functions⁴⁶ defined by $j^{\text{max}} = l^{\text{max}} = 22$ and $k^{\text{max}} = 12$. The resulting energy levels with $J = 0$ are well converged; however for WAVR4, calculations of the same accuracy for levels with $J = 1$ require about 10 times more computer time. This is a consequence of the J – K coupling used in the EKE procedure. This coupling allows the system to go smoothly from bent to linear geometries but has the consequence that the vibrational basis set becomes K -dependent (see ref 55 for a detailed discussion of this issue). This coupling is essential for the linear HCCH system⁵³ and very floppy molecules,⁴⁴ but not for H_2O_2 . The

use of WAVR4 to calculate energies of high J levels is computationally unrealistic at present, and we note that, indeed, corresponding studies on acetylene have thus far been confined to low J values.⁵⁶

TROVE⁴³ is a computer suite for rovibrational calculations of energies and intensities for molecules of (at least in principle) arbitrary structures. In this approach, the Hamiltonian operator is represented as an expansion around a (nonrigid) reference configuration, which in the present work is defined by the torsion mode associated with the dihedral angle τ . In the reference configuration the H_2O_2 molecule has bond lengths R , r_1 , and r_2 and bond angles θ_1 and θ_2 frozen at their equilibrium values and τ varying on a fine grid of τ_k ($k = 0 \dots 10000$) values ranging from 0° to 720° (see below). The kinetic energy operator is expanded around each reference geometry $\{R_e, r_e, \theta_e, \theta_e, \tau_k\}$ in terms of the five linearized coordinates, ξ_i ,⁵⁷

$$\xi_1 = R^I - R_e$$

$$\xi_2 = r_1^I - r_e$$

$$\xi_3 = r_2^I - r_e$$

$$\xi_4 = \theta_1^I - \theta_e$$

$$\xi_5 = \theta_2^I - \theta_e$$

where R^I , r_1^I , r_2^I , θ_1^I and θ_2^I are linearized versions of the internal coordinates R , r_1 , r_2 , θ_1 and θ_2 and $\xi_6 = \tau$ is the sixth coordinate (see Figure 1). The potential energy function is also expanded but using three Morse-type variables $[1 - \exp(-a_i \xi_i)]$ ($i = 1, 2, 3$) and two bending coordinates ξ_4 and ξ_5 . Here $a_1 = 2.2 \text{ \AA}^{-1}$, $a_2 = a_3 = 2.3 \text{ \AA}^{-1}$ were selected to match closely the shape of the ab initio PES along the stretching modes. The dependence of the Hamiltonian on the torsional coordinate $\xi_6 = \tau$ is treated explicitly as a $k = 0 \dots 10000$ grid of values.

The rovibrational motion of the nonrigid molecule HOOH is best represented by the extended $C_{2h}^+(M)$ molecular symmetry group,⁵⁸ which is isomorphic to $D_{2h}(M)$ as well as to the extended group $G4(EM)$.⁵⁷ As explained by Hougen,⁵⁸ the extended group is needed to describe the torsional splitting due both the cis and trans tunnelings. In the present work, we use the $D_{2h}(M)$ group to classify the symmetry of the HOOH states. This group is given by the eight irreducible representations $A_g, A_u, B_{1g}, B_{1u}, B_{2g}, B_{2u}, B_{3g}$ and B_{3u} . To account for the extended symmetry properties of the floppy HOOH molecules, an extended range for torsion motion, from 0° to 720° was introduced into TROVE. In this representation, $\tau = 0^\circ, 360^\circ$ and 720° correspond to the cis barrier, and at $\tau = 180^\circ$ and 540° , the molecule has the trans configuration. In principle, this allows us to resolve both the cis and trans splitting.

To construct the basis set, TROVE employs a multistep contraction scheme based on the following polyad truncation. We chose the polyad number in the case of H_2O_2 that is given by

$$P = 4\nu_1 + 8(\nu_2 + \nu_3) + 8(\nu_4 + \nu_5) + \nu_6 \quad (2)$$

where ν_i is a vibrational quantum number associated with a one-dimensional primitive basis function $\phi_{\nu_i}(\xi_i)$ ($i = 1, 2, 3, \dots, 6$). At the first step, six sets of $\phi_{\nu_i}(\xi_i)$ are generated using the Numerov–Cooley^{59,60} method by solving the 1D Schrödinger

equations for each of the six modes separately. The corresponding 1D Hamiltonian operators are obtained from the 6D Hamiltonian operator ($J = 0$) by freezing all vibrational coordinates but one at their equilibrium values. The integration ranges are selected to be large enough to accommodate all basis functions required (see below for the discussion of the basis set sizes). The torsional functions are obtained initially on the range $\tau = 0 \dots 360^\circ$ and transform according to the $C_{2h}(M)$ group. A very fine grid of 30 000 points and the quadruple numerical precision [real(16)] was used for generating the eigenfunctions of the corresponding Schrödinger equation to resolve the trans splittings up to $\nu_6 = 42$. The wave functions are then extended to $\tau = 360 \dots 720^\circ$ through the \pm reflection of the $C_{2h}(M)$ values and classified according to $D_{2h}(M)$. The extended primitive torsion functions are able to account for the torsional splitting due to both the cis and trans tunneling.

At the second step, the 6D coordinate space is divided into the four reduced subspaces: (1) $\{\xi_1\}$, (2) $\{\xi_2, \xi_3\}$, (3) $\{\xi_4, \xi_5\}$, and (4) $\{\xi_6\}$. This division is dictated by symmetry: each of the subspaces is symmetrically independent and, thus, can be processed separately. For each of these subspaces, the Schrödinger equations are solved for the corresponding reduced Hamiltonian operators employing as basis the products of the corresponding primitive functions $\phi_{\nu_i}(\xi_i)$ generated at the first step. The subspace bases are truncated using the condition $P \leq P_{\max}$ where P is given by eq 2. In this work, we use $P_{\max} = 42$ (see below); that is, according to eq 2, our reduced subspace basis sets are defined by

$$4\nu_1 \leq 42 \quad (3)$$

$$8(\nu_2 + \nu_3) \leq 42 \quad (4)$$

$$8(\nu_4 + \nu_5) \leq 42 \quad (5)$$

$$\nu_6 \leq 42 \quad (6)$$

The four sets of eigenfunctions, $\Psi_{\lambda_1}^{(1)}(\xi_1)$, $\Psi_{\lambda_2}^{(2)}(\xi_2, \xi_3)$, $\Psi_{\lambda_3}^{(3)}(\xi_4, \xi_5)$, and $\Psi_{\lambda_4}^{(4)}(\xi_6)$, resulting from these solutions are symmetrized according to $D_{2h}(M)$ (see below) and assigned local mode quantum numbers (1) ν_1 ; (2) ν_2, ν_3 ; (3) ν_4, ν_5 ; and (4) ν_6 and vibrational symmetry Γ_{vib} . The final vibrational basis set is formed from products $\Psi_{\lambda_1}^{(1)} \times \Psi_{\lambda_2}^{(2)} \times \Psi_{\lambda_3}^{(3)} \times \Psi_{\lambda_4}^{(4)}$, which are contracted with $P \leq 42$ and symmetrized in $D_{2h}(M)$ again using the standard technique for transformations to irreducible representations (see, for example, ref 57). Thus, our contracted vibrational basis set consists of eight symmetrically independent groups, one for each irreducible representation of the $D_{2h}(M)$ group $A_g, A_u, B_{1g}, B_{1u}, B_{2g}, B_{2u}, B_{3g}$ and B_{3u} . However, only four of them— A_g, A_u, B_{1g}, B_{1u} —correspond to the internal eigenfunctions with nonzero nuclear statistical weights and are thus physically meaningful. Therefore, for each J , only these four Hamiltonian matrices are constructed and diagonalized. In the diagonalizations, we use the eigensolver DSYEV from LAPACK as implemented in the MKL libraries.

Calculations using the program TROVE started with a search for the optimal values (i) of the size of the basis set (as controlled by P_{\max}) and (ii) of the operator expansion orders, which would give results close to the EKE ones. These parameters were chosen to meet two conflicting requirements: the best possible convergence and a compact enough calculation to allow high- J energy levels to be computed. The final value of the maximum polyad number P_{\max} was chosen at

Table 1. Calculated and Observed Energy Levels, in cm^{-1} , for $J = 0$ Published by Małyszczek and Koput (MK),¹⁶ Using WAVR4, TROVE, and RVIB4^a

ν_1	ν_2	ν_3	ν_4	ν_5	ν_6	sym	obs	MK	WAVR4	TROVE	TROVE*	RVIB4*
0	0	0	1	0	0	A_g	254.550	255.43	256.406	256.419	255.490	255.534
0	0	0	2	0	0	A_g	569.743	570.45	570.334	570.251	570.690	570.878
0	0	1	0	0	0	A_g	865.939	866.02	865.547	865.652	865.468	865.535
0	0	0	3	0	0	A_g	1000.882	1001.92	1001.227	1001.073	1002.493	1002.791
0	0	0	0	0	1	B_u	1264.583	1264.54	1264.819	1265.121	1264.868	1264.959
0	0	0	1	0	1	B_u	1504.872	1505.18	1505.977	1506.283	1505.634	1505.712
0	0	0	2	0	1	B_u	1853.634	1854.28	1853.949	1854.424	1855.305	1855.332
0	0	0	0	0	0	A_u	11.437	11.28	11.014	10.997	11.289	11.305
0	0	0	1	0	0	A_u	370.893	371.32	371.247	371.203	371.478	371.597
0	0	0	2	0	0	A_u	776.122	776.93	776.465	776.320	777.336	777.567
0	0	1	0	0	0	A_u	877.934	877.83	877.094	877.200	877.303	877.377
0	0	0	0	0	1	B_g	1285.121	1285.03	1284.889	1285.249	1285.457	1285.552
0	0	0	1	0	1	B_g	1648.367	1648.71	1648.553	1649.012	1649.485	1649.540
0	0	0	2	0	1	B_g	2072.404	2073.05	2072.384	2072.949	2074.231	2074.367

^aResults calculated, using TROVE and RVIB4,⁶⁶ marked with an asterism (*), are computed with an adjusted height for the torsional barrier. The observed values are taken from refs 35, 36, 67, and 68.

Table 2. Calculated and Observed Energy Levels, in cm^{-1} , for the Vibrational Ground State (left hand column) and the (000 100 A_g) State (right hand column) with $J = 1, 3$, and 5^a

J	K_a	K_c	obs	calcd	obs – calcd	obs	calcd	obs – calcd
1	0	1	1.71154	1.71152	0.00002	256.255	256.255	0.000
1	1	1	10.9068	10.9068	0.0000	265.427	265.427	0.000
1	1	0	10.9426	10.9426	0.0000	265.474	265.475	0.001
3	0	3	10.2683	10.2682	0.0001	264.777	264.777	0.000
3	1	3	19.374	19.374	0.000	273.830	273.831	–0.001
3	1	2	19.589	19.589	0.000	274.119	274.117	0.002
3	2	2	47.115	47.115	0.000	301.555	301.556	0.001
3	2	1	47.115	47.115	0.000	301.556	301.557	0.001
3	3	1	93.155	93.155	0.000	347.509	347.512	0.003
3	3	0	93.155	93.155	0.000	347.509	347.512	0.003
5	0	5	25.6667	25.6664	0.0003	280.113	280.112	0.001
5	1	5	34.613	34.613	0.000	288.954	288.954	0.000
5	1	4	35.151	35.150	0.001	289.671	289.671	0.000
5	2	4	62.513	62.513	0.000	316.893	316.893	0.000
5	2	3	62.517	62.517	0.000	316.899	316.899	0.000
5	3	3	108.551	108.551	0.000	362.845	362.847	0.002
5	3	2	108.551	108.551	0.000	362.845	362.847	0.002
5	4	2	172.968	172.968	0.000	427.143	427.146	0.003
5	4	1	172.968	172.968	0.000	427.143	427.146	0.003
5	5	1	255.733	255.733	0.000	509.757	509.764	0.007
5	5	0	255.733	255.733	0.000	509.757	509.764	0.007

^aObserved energy levels taken from ref 36.

42, which is also the highest excitation of the torsional mode ν_6 (see eq 6). For the OO stretch, the maximal excitation number was 8; for OH stretches, –8; and for the bending modes, –10 (see eqs 2 and 3–5). These parameters control the size of the basis set used in the TROVE calculations according to the multistep contraction approach described above. For the $J = 0$ levels, these values give good agreement with other methods (see Table 1). The kinetic energy operator and potential energy function were represented by sixth- and eighth-order expansions, respectively.

RESULTS

The updated version of TROVE was used to calculate excited rotational levels for J up to 35, the highest assigned thus far experimentally. Initial calculations were performed with the

equilibrium distances and angles obtained ab initio in ref 16. In this case, the discrepancies between theory and experiment increased quadratically with increasing J : the $J = 1$ levels were calculated with an accuracy around 0.001 cm^{-1} , but those for $J = 35$ differ from experiment by about 1 cm^{-1} .

We therefore chose to adjust the equilibrium parameters R_e and r_e to better reproduce the experimental values. Only very small changes were needed to make the $J = 35$ levels accurate to about 0.03 cm^{-1} for the ground vibrational state. In particular, the original value of R_e of $1.455\,393\,78 \text{ Å}$ was shifted to $1.455\,777\,28 \text{ Å}$ and $r_e = 0.962\,524\,76 \text{ Å}$ moved to $0.962\,530\,06 \text{ Å}$. The rotational structure within the excited vibrational states is of similar accuracy, meaning that these levels are essentially shifted by just the discrepancy in the vibrational band origin. In practice, this geometry shift not only meant that low J energy

Table 3. Calculated and Observed Energy Levels, in cm^{-1} , for the (000 200 A_g) (left hand column) and the (000 300 A_g) State (right hand column) with $J = 1, 3$, and S^a

J	K_a	K_c	obs	calcd	obs – calcd	obs	calcd	obs – calcd
1	0	1	571.448	571.449	−0.001	1002.584	1002.584	0.000
1	1	1	580.550	580.549	0.001	1011.664	1011.614	0.050
1	1	0	580.577	580.576	0.001	1011.678	1011.628	0.050
3	0	3	579.976	579.975	0.001	1011.098	1011.097	0.001
3	1	3	589.009	589.007	0.002	1020.143	1020.093	0.050
3	1	2	589.174	589.172	0.002	1020.225	1020.176	0.049
3	2	2	616.427	616.427	0.000	1047.246	1047.244	0.002
3	2	1	616.427	616.427	0.000	1047.246	1047.244	0.002
3	3	1	661.974	661.975	0.001	1092.462	1092.411	0.051
3	3	0	661.974	661.975	0.001	1092.462	1092.411	0.051
5	0	5	595.324	595.324	0.000	1026.421	1026.021	0.008
5	1	5	604.235	604.232	0.003	1035.404	1035.354	0.050
5	1	4	604.645	604.644	0.001	1035.610	1035.561	0.049
5	2	4	631.773	631.773	0.000	1062.566	1062.565	0.001
5	2	3	631.775	631.775	0.000	1062.566	1062.565	0.001
5	3	3	677.317	677.315	0.002	1107.779	1107.729	0.050
5	3	2	677.317	677.315	0.002	1107.779	1107.729	0.050
5	4	2	741.046	741.044	0.002	1170.935	1170.930	0.005
5	4	1	741.046	741.044	0.002	1170.935	1170.930	0.005
5	5	1	822.934	822.930	0.004	1252.191	1252.140	0.051
5	5	0	822.934	822.930	0.004	1252.191	1252.140	0.051

^aObserved energy levels taken from ref 36.

Table 4. Calculated and Observed Energy Levels, in cm^{-1} , for the (001 000 A_g) (left hand column) and the (000 000 A_u) State (right hand column) with $J = 1, 3$, and S^a

J	K_a	K_c	obs	calcd	obs – calcd	obs	calcd	obs – calcd
1	0	1	867.628	867.628	0.000	13.150	13.149	0.001
1	1	1	876.815	876.816	0.001	22.337	22.337	0.000
1	1	0	876.851	876.850	0.001	22.369	21.368	0.001
3	0	3	876.074	875.073	0.001	21.712	21.711	0.001
3	1	3	885.171	884.171	0.000	30.821	30.820	0.001
3	1	2	885.386	885.387	−0.001	31.009	31.009	0.000
3	2	2	912.886	912.885	0.001	58.518	58.518	0.000
3	2	1	912.887	912.887	0.000	58.518	58.518	0.000
3	3	1	958.884	958.887	−0.003	104.508	104.508	0.000
3	3	0	958.884	958.887	−0.003	104.508	104.508	0.000
5	0	5	891.273	891.2712	0.002	37.121	37.120	0.001
5	1	5	900.210	900.209	0.001	46.089	46.088	0.001
5	1	4	900.749	900.748	0.001	46.561	46.560	0.001
5	2	4	928.085	928.085	0.000	73.926	73.926	0.000
5	2	3	928.089	928.088	0.001	73.929	73.928	0.001
5	3	3	974.080	974.082	−0.002	119.913	119.913	0.000
5	3	2	974.080	974.082	−0.002	119.913	119.913	0.000
5	4	2	1038.438	1038.440	−0.002	184.260	184.261	−0.001
5	5	1	1121.127	1121.133	−0.006	266.936	266.938	−0.002

^aObserved energy levels taken from ref 36.

levels were reproduced with an accuracy of 1 cm^{-1} , reproducing the accuracy of the vibrational band origin, but also resulted in pseudoresonance artifacts. To illustrate this, consider the interaction between the ground vibrational state and the low-lying $\nu_4 = 1$ torsional vibrational state, which lies about 2 cm^{-1} too low in the calculations. This results in an artificial closeness and interaction between levels with the same J and $K_a = 8$ for $\nu = 0$ and $K_a = 6$ for $\nu_4 = 1$. The resulting shift in the energy levels is significant; it grows with J and reaches about 1 cm^{-1} at $J = 30$. We call this a pseudoresonance artifact since no such

interaction is seen in the experimentally determined energy levels.

There are several ways to avoid this artificial pseudoresonance. One would be to fit the PES to experimental data, which would remove this artificial near-degeneracy. This is likely to be a topic of future work. An alternative possibility, which is already available within TROVE,³⁷ is to simply adjust the calculated values of the vibrational band origins given by the $J = 0$ calculation to the observed ones prior to their use in calculations of the $J > 0$ levels. This option, which is not available in EKE codes that couple the bending basis with the

Table 5. Calculated and Observed Energy Levels, in cm^{-1} , for the (000 100 A_u) (left hand column) and the (000 200 A_u) State (right hand column) with $J = 1, 3$, and 5^a

J	K_a	K_c	obs	calcd	obs – calcd	obs	calcd	obs – calcd
1	0	0	372.601	372.602	0.001	777.826	777.827	–0.001
1	1	1	381.733	381.733	0.000	786.881	786.891	–0.010
1	1	0	381.764	381.764	0.000	786.901	786.911	–0.010
3	0	3	381.140	381.139	0.001	786.350	786.350	0.000
3	1	3	390.195	390.195	0.000	795.355	795.365	–0.010
3	1	2	390.378	390.376	0.002	795.472	795.482	–0.010
3	2	2	417.723	417.722	0.001	822.639	822.640	–0.001
3	2	1	417.723	417.722	0.001	822.639	822.640	–0.001
3	3	1	463.434	463.434	0.000	867.976	867.986	–0.010
3	3	0	463.434	463.434	0.000	867.976	867.986	–0.010
5	0	5	396.505	396.504	0.001	801.689	801.689	0.000
5	1	5	405.426	405.423	0.003	810.607	810.617	–0.010
5	1	4	405.881	405.879	0.002	810.900	810.909	–0.009
5	2	4	433.088	433.088	0.000	837.977	837.977	0.000
5	2	3	433.090	433.089	0.001	837.977	837.977	0.000
5	3	3	478.796	478.794	0.002	883.310	883.320	–0.010
5	3	2	478.796	478.794	0.002	883.310	883.320	–0.010
5	4	2	542.756	542.756	0.000	946.769	946.770	0.001
5	5	1	624.938	624.937	0.001	1028.289	1028.299	–0.010

^aObserved energy levels taken from the Ref 36.

Table 6. Calculated and Observed Energy Levels, in cm^{-1} , for the (000 001 B_g) state (left-hand column) and the (000 101 B_u) state (right-hand column) with $J = 1, 3$, and 5^a

J	K_a	K_c	obs	calcd	obs – calcd	obs	calcd	obs – calcd
1	0	1	1266.28407	1266.28438	–0.00031	1506.56787	1506.5802	–0.012
1	1	1	1275.63614	1275.63712	–0.00098	1515.88545	1515.8860	–0.001
1	1	0	1275.68143	1275.68147	0.00004	1515.93499	1515.9356	0.000
3	0	3	1274.78856	1274.77878	0.0098	1515.04966	1515.04938	0.000
3	1	3	1284.03134	1284.03029	0.0010	1524.24322	1524.24215	0.001
3	1	2	1284.29658	1284.29626	0.0003	1524.54079	1524.53972	0.001
3	2	2	1312.28218	1312.28131	0.0009	1552.41136	1552.40795	0.004
3	2	1	1312.28254	1312.28139	0.0011	1552.41246	1552.40897	0.004
3	3	1	1359.12820	1359.12545	0.0028	1599.09294	1599.08566	0.008
3	3	0	1359.12820	1359.12552	0.0028	1599.09294	1599.08566	0.008
5	0	5	1290.09145	1290.08916	0.002	1530.31072	1530.31766	–0.007
5	1	5	1299.13927	1299.13530	0.004	1539.28527	1539.28077	0.005
5	1	4	1299.80285	1299.80038	0.002	1540.02903	1540.02446	0.005
5	2	4	1327.58442	1327.58155	0.003	1567.67490	1567.66816	0.007
5	2	3	1327.59029	1327.58677	0.003	1567.68116	1567.67872	0.003
5	3	3	1374.42901	1374.42459	0.005	1614.35427	1614.35453	0.009
5	3	2	1374.42901	1374.42466	0.005	1614.35427	1614.35453	0.009
5	4	2	1439.96732	1439.96148	0.006	1679.66574	1679.66148	0.004
5	4	1	1439.96732	1439.96150	0.006	1679.66574	1679.66148	0.004
5	5	1	1524.16347	1524.15611	0.007	1763.57628	1763.56600	0.010
5	5	0	1524.16347	1524.15611	0.007	1763.57628	1763.56600	0.010

^aObserved energy levels taken from ref 35.

rotational functions,⁵⁵ not only shifts the energies, it also rearranges the matrix elements so that the artificial resonances disappear. With this adjusted calculation, the energy levels vary smoothly with the increasing J and K_a quantum numbers (see Tables 6, 8, and 10), as one would expect⁶¹ from purely ab initio levels.

One other problem remained when comparing our rotationally excited energy levels with the observed ones. This concerned rotational levels with the quantum number $K_a = 1$ that did not behave as levels associated with other values of K_a . The error for the two levels with $K_a = 1$ increases

disproportionately to that of other levels as J increases. This error was about 0.1 cm^{-1} for $J = 30$. A series of test calculations revealed the reason for such discrepant behavior of the levels with $K_a = 1$. It happens that a small change in the height of the torsional barrier, which is strongly influenced by the linear expansion coefficient c_{000001} , does not affect other K_a levels, but significantly influences only those with $K_a = 1$. Varying this expansion coefficient can both increase and decrease the splitting of the $K_a = 1$ doublet. Because this splitting is overestimated in calculations using the ab initio value of c_{000001} , its reduction by about 1% from the ab initio value of 0.004 87

Table 7. Calculated and Observed Energy Levels, in cm^{-1} , for the (000 201 B_u) (left hand column) and the (000 001 B_g) State (right hand column) with $J = 1, 3$, and 5^a

J	K_a	K_c	obs	calcd	obs – calcd	obs	calcd	obs – calcd
1	0	1	1855.33138	1855.3313	0.00005	1286.82243	1286.82339	0.0009
1	1	1	1864.55771	1864.5582	–0.0005	1296.15883	1296.15986	–0.001
1	1	0	1864.58570	1864.586	–0.0003	1296.19549	1296.19702	–0.002
3	0	3	1863.81707	1863.815	0.002	1295.33667	1295.335	0.001
3	1	3	1872.97340	1872.977	–0.004	1304.57897	1304.578	0.050
3	1	2	1873.14226	1873.142	0.000	1304.80087	1304.801	0.049
3	2	2	1900.77501	1900.777	–0.002	1332.74677	1332.747	0.002
3	2	1	1900.77501	1900.777	–0.002	1332.74977	1332.748	0.002
3	3	1	1946.95101	1946.955	–0.004	1379.49078	1379.491	0.051
3	3	0	1946.95101	1946.955	–0.004	1379.49078	1379.411	0.051
5	0	5	1879.08915	1879.084	0.005	1310.65278	1310.652	0.000
5	1	5	1888.11891	1888.112	0.007	1319.73145	1319.730	0.001
5	1	4	1888.54189	1888.544	–0.002	1320.28562	1320.287	–0.001
5	2	4	1916.04590	1916.044	0.002	1348.06457	1348.064	0.000
5	2	3	1916.04847	1916.045	0.003	1348.06876	1348.068	0.000
5	3	3	1962.22103	1962.225	–0.004	1394.80562	1394.805	0.000
5	3	2	1962.22103	1962.222	–0.004	1394.80562	1394.805	0.000
5	4	2	2026.82112	2026.824	–0.003	1460.20415	1460.204	0.000
5	4	1	2026.82112	2026.824	–0.003	1460.20415	1460.204	0.000
5	5	1	2109.84480	2109.840	0.005	1544.22243	1544.223	–0.001
5	5	0	2109.84480	2109.840	0.005	1544.22243	1544.223	–0.001

^aObserved energy levels taken from ref 35.**Table 8. Calculated and Observed Energy Levels, in cm^{-1} , for $J = 30^a$**

J	K_a	K_c	obs	calcd	obs – calcd	obs	calcd	obs – calcd
30	0	30	789.577	789.581	–0.004	1038.983	1038.925	0.058
30	1	30	793.053	793.065	–0.012	1041.540	1041.481	0.039
30	1	29	809.594	809.565	0.029	1063.053	1063.007	0.046
30	2	29	829.292	829.282	0.010	1080.396	1080.345	0.051
30	2	28	832.547	832.521	0.026	1086.079	1086.036	0.043
30	3	28	876.030	876.017	0.013	1127.862	1127.815	0.047
30	3	27	876.191	876.174	0.017	1128.304	1128.262	0.042
30	4	27	940.027	940.015	0.012	1191.838	1191.794	0.044
30	4	26	940.029	940.013	0.016	1191.850	1191.807	0.043
30	5	26	1022.323	1022.311	0.012	1274.332	1274.293	0.039
30	5	25	1022.324	1022.312	0.012	1274.332	1274.293	0.039
30	6	25	1122.848	1122.837	0.011	1371.047	1371.024	0.023
30	6	24	1122.849	1122.838	0.011	1371.047	1371.024	0.023
30	7	24	1241.304	1241.294	0.010	1491.957	1491.933	0.024
30	7	23	1241.304	1241.294	0.010	1491.957	1491.933	0.024
30	8	23	1381.938	1381.916	0.022	1628.749	1628.731	0.018
30	9	21	1534.588	1534.578	0.010	1782.735	1782.739	–0.004
30	10	21	1707.358	1707.349	0.009	1958.577	1958.558	0.019
30	11	19	1898.169	1898.159	0.010	2148.182	2148.186	–0.004

^aResults are for the ground vibrational state (left hand column) and the (000 100 A_g) state - (right hand column). Observed energy levels taken from ref 36.

to $0.00483 E_h$ results in roughly a 4-fold improvement of the obs – calc value for the $K_a = 1$ levels. This change affects the value of the ground-state torsional splitting of 11 cm^{-1} and also the values of the other torsional energy levels, all of which move significantly closer to the observed values than the purely ab initio levels given in Table 1. In particular, this small adjustment improves the calculated ground-state splitting to 11.4 cm^{-1} and the first torsional level to 255.2 cm^{-1} . Thus, adjusting c_{000001} not only significantly improves the values of levels with $K_a = 1$, it also improves the overall agreement with experiment for the band origins. The underlying reason for this is that the

expansion coefficient c_{000001} controls the height of the torsional barrier.

These minor adjustments result in very accurate values for rotational energy levels, a sample of which are presented in Tables 2–7. For the experimentally “observed” energy levels, we have used the levels tabulated by refs 35 and 36, which were actually calculated using an effective Hamiltonian model. In all cases considered, these models reproduce the measurements within experimental error; however, for the higher J levels considered, an increasing proportion of the levels are actually predictions of the model and were not measured. Thus, for

Table 9. Calculated and Observed Energy Levels, in cm^{-1} , for $J = 30$ Levels of the (000 000 A_u) Vibrational State^a

J	K_a	K_c	obs	calcd	obs – calcd
30	0	30	802.349	802.340	0.009
30	1	30	806.280	806.276	0.004
30	1	29	820.768	820.746	0.022
30	2	29	841.344	841.330	0.013
30	2	28	843.911	843.892	0.019
30	3	28	887.854	887.839	0.015
30	3	27	887.964	887.949	0.015
30	4	27	951.826	951.815	0.011
30	4	26	951.828	951.817	0.011
30	5	26	1034.096	1034.085	0.011
30	5	25	1034.096	1034.085	0.011
30	5	25	1134.609	1134.599	0.010
30	5	24	1253.291	1253.284	0.007
30	5	24	1390.060	1390.055	0.005
30	5	23	1544.803	1544.803	0.000
30	5	23	1717.164	1717.167	–0.003

^aObserved energy levels taken from ref 36.

Table 10, only the levels $35_{6,29}$ at 1402.369 cm^{-1} and $35_{8,29}$ at 1662.739 cm^{-1} actually correspond to levels that have been directly measured; however, our comparisons show no difference in the agreement between measured and predicted levels, confirming the accuracy of the predictions. A more comprehensive set of energy levels is given in the Supporting Information. Since the cis splitting is extremely small, generally less than our convergence error, we have not attempted to separately identify this effect of tunneling.

From the various tables, one can see that the discrepancy between observed and calculated energy values increases both gently and smoothly with rotational quantum number J . Such calculations therefore provide an excellent starting point for assigning high- J transitions both within the ground state and to excited vibrational states, as the density of observed transitions is orders of magnitude smaller than the accuracy of calculations.

CONCLUSIONS

We present results of ab initio and slightly adjusted ab initio calculations for the vibrational and rovibrational energy levels of the H_2O_2 molecule. Use of the accurate ab initio PES calculated by Malyszczek and Koput¹⁶ reproduces the known vibrational band origin with a standard deviation of $\sim 1 \text{ cm}^{-1}$. The use of the program TROVE⁴³ for the nuclear motion calculations allowed us to compute high rotational levels up to $J = 35$. Indeed, energy levels with $J = 50$ could be calculated on a high-end workstation, and the accuracy of prediction will be very high: better than 0.5 cm^{-1} . However, we have not yet performed such calculations because no comparison with experimental values is currently possible. Experimentally derived energy levels up to $J = 35$ are compared with our calculations. These are reproduced with an unprecedented accuracy of 0.001 cm^{-1} for the levels up to $J = 10$ and 0.02 cm^{-1} for all the known levels above this. Variational calculations using this slightly adjusted ab initio PES results in very smooth variation in the discrepancies between the observed and calculated levels as a function of the rotational quantum numbers J and K_a . This smoothness and accuracy is the key to the successful analysis of previously unassignable spectra^{30,61} because, in particular, the accidental resonances, which seriously complicate any analysis based on the use an effective Hamiltonian, are automatically allowed for in such calculations.

There is one other important aspect of the H_2O_2 rotation-vibration problem that we should mention. The detection of extrasolar planets and, in particular, our ability to probe the molecular composition of these bodies using spectroscopy⁶² has led to demand for accurate, comprehensive line lists over an extended range of both temperature and wavelength for all species of possible importance in exoplanet atmospheres.⁶³ The accuracy of the calculations presented here and, especially, their ability to reliably predict highly excited rotational levels which are of increasing importance at higher temperatures suggest that the present work will provide an excellent starting point for the calculation of a comprehensive line list for H_2O_2 . In this, we will be following the recent work of Bowman and co-workers, who have computed similar line lists for somewhat more rigid hydrocarbon systems.^{64,65}

Table 10. Variationally Calculated and Observed or (Predicted Using Effective Hamiltonian) Energy Levels, in cm^{-1} , for $J = 35^a$

J	K_a	K_c	obs	calcd	obs – calcd	obs	calcd	obs – calcd
35	0	35	1067.027	1067.037	–0.010	1314.205	1314.124	0.081
35	1	35	1069.466	1069.484	–0.018	1315.869	1315.787	0.082
35	1	34	1091.715	1091.680	0.035	1344.395	1344.338	0.057
35	2	34	1108.893	1108.882	0.011	1358.709	1358.637	0.052
35	2	33	1114.564	1114.523	0.041	1368.256	1368.203	0.053
35	3	33	1156.257	1156.241	0.016	1407.374	1407.309	0.065
35	3	32	1156.655	1156.628	0.027	1408.434	1408.382	0.052
35	4	32	1220.062	1220.044	0.018	1471.314	1471.252	0.062
35	4	31	1220.070	1220.051	0.019	1471.355	1471.296	0.059
35	5	31	1302.102	1302.088	0.014	1553.875	1553.821	0.054
35	5	30	1302.114	1302.098	0.016	1553.876	1555.822	0.054
35	6	30	1402.366	1402.353	0.013	1648.318	1648.288	0.030
35	6	29	1402.369	1402.350	0.019	1648.318	1648.288	0.030
35	7	29	1520.294	1520.282	0.012	1769.879	1769.844	0.035
35	8	28	1662.739	1662.707	0.032	1906.483	1906.459	0.024
35	9	27	1814.222	1814.207	0.015			
35	10	26	1986.565	1986.552	0.013			

^aObserved energy levels taken from the ref 36.

Table 11. Variationally Calculated and Observed or (Predicted Using Effective Hamiltonian) Energy Levels, in cm^{-1} , for $J = 35$

J	K_a	K_c	obs	calcd	obs – calcd	obs	calcd	obs – calcd
35	0	35	1933.163	1932.118	0.045	1080.587	1080.574	0.013
35	1	35	1936.042	1935.996	0.046	1083.472	1083.465	0.007
35	1	34	1955.496	1955.415	0.081 u	1102.961	1102.929	0.032
35	2	34	1973.810	1973.743	0.067 u	1121.270	1121.247	0.023
35	2	33	1978.296	1978.228	0.068 u	1125.774	1125.743	0.031
35	3	33	2020.807	2020.749	0.058 u	1168.268	1168.245	0.023
35	3	32	2021.078	2021.020	0.058 u	1168.540	1168.517	0.023
35	4	32	2084.733	2084.691	0.042 u	1232.076	1232.060	0.016
35	4	31	2084.738	2084.768	0.042 u	1232.081	1232.055	0.026
35	5	31	2165.503	2165.420	0.083 u	1314.156	1314.138	0.018
35	5	30	2165.503	2165.420	0.083 u	1314.156	1314.138	0.018
						1414.475	1414.459	0.016
						1532.940	1532.928	0.012
						1669.447	1669.438	0.009
						1823.841	1823.839	0.002

■ ASSOCIATED CONTENT

● Supporting Information

Expansion coefficients, c_{ijklmn} used to describe the potential given in eq 1 and a more comprehensive set of rovibrational energy levels than those provided in Tables 2–8. This information is available free of charge via the Internet at <http://pubs.acs.org>.

■ AUTHOR INFORMATION

Corresponding Author

*E-mail: j.tennyson@ucl.ac.uk.

Notes

The authors declare no competing financial interest.

■ ACKNOWLEDGMENTS

This work was performed as part of ERC Advanced Investigator Project 267219. We also thank the Russian Fund for Fundamental Studies for their support for aspects of this project.

■ REFERENCES

- (1) Davis, D. D. Kinetics review of atmospheric reactions involving H_2O_2 compounds. *Can. J. Chem.* **1974**, *52*, 1405–1414.
- (2) Vione, D.; Maurino, V.; Minero, C.; Pelizzetti, E. The atmospheric chemistry of hydrogen peroxide: A review. *Atmos. Environ.* **2003**, *37*, 477–488.
- (3) Allen, N. D. C.; Abad, G. G.; Bernath, P. F.; Boone, C. D. Satellite observations of the global distribution of hydrogen peroxide (H_2O_2) from ACE. *J. Quant. Spectrosc. Radiat. Transfer* **2013**, *115*, 66–77.
- (4) Encrenaz, T.; Bezaud, B.; Greathouse, T. K.; Richter, M. J.; Lacy, J. H.; Atreya, S. K.; Wong, A. S.; Lebonnois, S.; Lefevre, F.; Forget, F. Hydrogen peroxide on Mars: Evidence for spatial and seasonal variations. *Icarus* **2004**, *170*, 424–429.
- (5) Encrenaz, T.; Greathouse, T. K.; Lefevre, F.; Atreya, S. K. Hydrogen peroxide on Mars: Observations, interpretation and future plans. *Planet Space Sci.* **2012**, *68*, 3–17.
- (6) Bergman, P.; Parise, B.; Liseau, R.; Larsson, B.; Olofsson, H.; Menten, K. M.; Güsten, R. Detection of interstellar hydrogen peroxide. *Astron. Astrophys.* **2011**, *531*, L8.
- (7) Bramley, M. J.; Carrington, T. A general discrete variable method to calculate vibrational-energy levels of 3-atom and 4-atom molecules. *J. Chem. Phys.* **1993**, *99*, 8519–8541.
- (8) Carter, S.; Handy, N. C. The vibrations of H_2O_2 , studied by “multimode,” with a large amplitude motion. *J. Chem. Phys.* **2000**, *113*, 987–993.
- (9) Luckhaus, D. 6D vibrational quantum dynamics: Generalized coordinate discrete variable representation and (a)diabatic contraction. *J. Chem. Phys.* **2000**, *113*, 1329–1347.
- (10) Chen, R. Q.; Ma, G. B.; Guo, H. Six-dimensional quantum calculations of highly excited vibrational energy levels of hydrogen peroxide and its deuterated isotopomers. *J. Chem. Phys.* **2001**, *114*, 4763–4774.
- (11) Yu, H. G.; Muckerman, J. T. A general variational algorithm to calculate vibrational energy levels of tetraatomic molecules. *J. Mol. Spectrosc.* **2002**, *214*, 11–20.
- (12) Mladenovic, M. Discrete variable approaches to tetraatomic molecules Part II: application to H_2O_2 and H_2CO . *Spectrochim. Acta, Part A* **2002**, *58*, 809–824.
- (13) Lin, S. Y.; Guo, H. Exact quantum mechanical calculations of rovibrational energy levels of hydrogen peroxide (HOOH). *J. Chem. Phys.* **2003**, *119*, 5867–5873.
- (14) Carter, S.; Handy, N. C.; Bowman, J. M. High torsional vibrational energies of H_2O_2 and CH_3OH studied by MULTIMODE with a large amplitude motion coupled to two effective contraction schemes. *Mol. Phys.* **2009**, *107*, 727–737.
- (15) Carter, S.; Sharma, A. R.; Bowman, J. M. Multimode calculations of rovibrational energies and dipole transition intensities for polyatomic molecules with torsional motion: Application to H_2O_2 . *J. Chem. Phys.* **2011**, *135*, 014308.
- (16) Malyszczek, P.; Koput, J. Accurate ab initio potential energy surface and vibration-rotation energy levels of hydrogen peroxide. *J. Comput. Chem.* **2013**, *34*, 337–345.
- (17) Harding, L. B. Theoretical studies of the hydrogen peroxide potential energy surface 2. An ab initio, long-range $\text{OH}(^2\Pi) + \text{OH}(^2\Pi)$ potential. *J. Phys. Chem.* **1991**, *95*, 8653–8660.
- (18) Kuhn, B.; Rizzo, T. R.; Luckhaus, D.; Quack, M.; Suhm, M. A. A new six-dimensional analytical potential up to chemically significant energies for the electronic ground state of hydrogen peroxide. *J. Chem. Phys.* **1999**, *111*, 2565–2587.
- (19) Senent, M.; Fernandez-Herrera, S.; Smeyers, Y. Ab initio determination of the roto-torsional energy levels of hydrogen peroxide. *Spectrochim. Acta, Part A* **2000**, *56*, 1457–1468.
- (20) Koput, J.; Carter, S.; Handy, N. C. Potential energy surface and vibrational-rotational energy levels of hydrogen peroxide. *J. Phys. Chem. A* **1998**, *102*, 6325–6335.
- (21) Ticich, T. M.; Rizzo, T. R. *J. Chem. Phys.* **1986**, *84*, 1508–1520.
- (22) Polyansky, O. L.; Császár, A. G.; Shirin, S. V.; Zobov, N. F.; Barletta, P.; Tennyson, J.; Schwenke, D. W.; Knowles, P. J. High accuracy ab initio rotation-vibration transitions of water. *Science* **2003**, *299*, 539–542.
- (23) Pavanello, M.; Adamowicz, L.; Alijah, A.; Zobov, N. F.; Mizus, I. I.; Polyansky, O. L.; Tennyson, J.; Szidarovszky, T.; Császár, A. G.; Berg, M.; et al. Precision measurements and computations of transition

energies in rotationally cold triatomic hydrogen ions up to the mid-visible spectral range. *Phys. Rev. Lett.* **2012**, *108*, 023002.

(24) Huang, X.; Schwenke, D. W.; Tashkun, S. A.; Lee, T. J. An isotopic-independent highly-accurate potential energy surface for CO₂ isotopologues and an initial ¹²C¹⁶O₂ IR line list. *J. Chem. Phys.* **2012**, *136*, 124311.

(25) Huang, X.; Schwenke, D. W.; Lee, T. J. Rovibrational spectra of ammonia. Part I: Unprecedented accuracy of a potential energy surface used with nonadiabatic corrections. *J. Chem. Phys.* **2011**, *134*, 044320.

(26) Huang, X.; Schwenke, D. W.; Lee, T. J. Rovibrational spectra of ammonia. Part II: Detailed analysis, comparison, and prediction of spectroscopic assignments for ¹⁴NH₃, ¹⁵NH₃, and ¹⁴ND₃. *J. Chem. Phys.* **2011**, *134*, 044321.

(27) Drossart, P.; Maillard, J. P.; Caldwell, J.; Kim, S. J.; Watson, J. K. G.; Majewski, W. A.; Tennyson, J.; Miller, S.; Atreya, S.; Clarke, J.; et al. Detection of H₃⁺ on Jupiter. *Nature* **1989**, *340*, 539–541.

(28) Lee, S. S.; Ventrudo, B. F.; Cassidy, D. T.; Oka, T.; Miller, S.; Tennyson, J. Observation of the 3ν₂ ← 0 overtone band of H₃⁺. *J. Mol. Spectrosc.* **1991**, *145*, 222–224.

(29) Dinelli, B. M.; Neale, L.; Polyansky, O. L.; Tennyson, J. New assignments for the infrared spectrum of H₃⁺. *J. Mol. Spectrosc.* **1997**, *181*, 142–150.

(30) Polyansky, O. L.; Zobov, N. F.; Viti, S.; Tennyson, J.; Bernath, P. F.; Wallace, L. Water in the sun: line assignments based on variational calculations. *Science* **1997**, *277*, 346–349.

(31) Polyansky, O. L.; Zobov, N. F.; Viti, S.; Tennyson, J. Water vapour line assignments in the near infrared. *J. Mol. Spectrosc.* **1998**, *189*, 291–300.

(32) Zumwalt, L. A.; Giguere, P. A. The infra-red bands of hydrogen peroxide at λ9720 and the structure and torsional oscillation of hydrogen peroxide. *J. Chem. Phys.* **1941**, *9*, 458–462.

(33) Giguere, P. A. The infra-red spectrum of hydrogen peroxide. *J. Chem. Phys.* **1950**, *18*, 88–92.

(34) Olson, W. B.; Hunt, R. H.; Young, B. W.; Maki, A. G.; Brault, J. W. Rotational constants of the lowest torsional component (0G) of the ground state and lowest torsional component (1G) of the first excited torsional state of hydrogen peroxide. *J. Mol. Spectrosc.* **1988**, *127*, 12–34.

(35) Perrin, A.; Flaud, J.-M.; Camy-Peyret, C.; Goldman, A.; Murcray, F. J.; Blatherwick, R. D. New analysis of the ν₆ band of H₂O₂ – the (n, τ) = (0, 1), (1, 1), (2, 1), (0, 3), and (1, 3) torsional subbands. *J. Mol. Spectrosc.* **1990**, *142*, 129–147.

(36) Camy-Peyret, C.; Flaud, J.-M.; Johns, J. W. C.; Noel, M. Torsion-vibration interaction in H₂O₂: First high-resolution observation of ν₃. *J. Mol. Spectrosc.* **1992**, *155*, 84–104.

(37) Yurchenko, S. N.; Barber, R. J.; Yachmenev, A.; Thiel, W.; Jensen, P.; Tennyson, J. A variationally computed T = 300 K line list for NH₃. *J. Phys. Chem. A* **2009**, *113*, 11845–11855.

(38) Yurchenko, S. N.; Barber, R. J.; Tennyson, J. A variationally computed hot (up to T = 1500 K) line list for NH₃. *Mon. Not. R. Astron. Soc.* **2011**, *413*, 1828–1834.

(39) Sung, K.; Brown, L. R.; Huang, X.; Schwenke, D. W.; Lee, T. J.; Coy, S. L.; Lehmann, K. K. Extended line positions, intensities, empirical lower state energies and quantum assignments of NH₃ from 6300 to 7000 cm⁻¹. *J. Quant. Spectrosc. Radiat. Transfer* **2012**, *113*, 1066–1083.

(40) Zobov, N. F.; Shirin, S. V.; Ovsyannikov, R. I.; Polyansky, O. L.; Yurchenko, S. N.; Barber, R. J.; Tennyson, J.; Hargreaves, R.; Bernath, P. Analysis of high temperature ammonia spectra from 780 to 2100 cm⁻¹. *J. Mol. Spectrosc.* **2011**, *269*, 104–108.

(41) Down, M. J.; Hill, C.; Yurchenko, S. N.; Tennyson, J.; Brown, L. R.; Kleiner, I. Assignment and labelling of experimental ammonia spectra: correcting and completing the HITRAN NH₃ database. *J. Quant. Spectrosc. Radiat. Transfer* **2013**.

(42) Carter, S.; Bowman, J. M. The adiabatic rotation approximation for rovibrational energies of many-mode systems: Description and tests of the method. *J. Chem. Phys.* **1998**, *108*, 4397–4404.

(43) Yurchenko, S. N.; Thiel, W.; Jensen, P. Theoretical ROVibational Energies (TROVE): A robust numerical approach to the

calculation of rovibrational energies for polyatomic molecules. *J. Mol. Spectrosc.* **2007**, *245*, 126–140.

(44) Kozin, I. N.; Law, M. M.; Hutson, J. M.; Tennyson, J. The rovibrational bound states of Ar₂HF. *J. Chem. Phys.* **2003**, *118*, 4896–4904.

(45) Lodi, L.; Tennyson, J.; Polyansky, O. L. A global, high accuracy ab initio dipole moment surface for the electronic ground state of the water molecule. *J. Chem. Phys.* **2011**, *135*, 034113.

(46) Kozin, I. N.; Law, M. M.; Tennyson, J.; Hutson, J. M. New vibration–rotation code for tetraatomic molecules WAVR4. *Comput. Phys. Commun.* **2004**, *163*, 117–131.

(47) Koput, J.; Carter, S.; Handy, N. C. Ab initio prediction of the vibrational-rotational energy levels of hydrogen peroxide and its isotopomers. *J. Chem. Phys.* **2001**, *115*, 8345–8350.

(48) Cizek, J. On the correlation problem in atomic and molecular systems. calculation of wavefunction components in Ursell-type expansion using quantum-field theoretical methods. *J. Chem. Phys.* **1966**, *45*, 4256–4266.

(49) Scuseria, G.; Lee, T. Comparison of coupled-cluster methods which include the effects of connected triple excitations. *J. Chem. Phys.* **1990**, *93*, 5851–5855.

(50) Noga, J.; Kutzelnig, W. Coupled cluster theory that takes care of the correlation cusp by inclusion of linear terms in the interelectronic coordinates. *J. Chem. Phys.* **1994**, *101*, 7738–7762.

(51) Werner, H. J.; Knowles, P. J.; Lindh, R.; Manby, F. R.; Schütz, M. MOLPRO, a package of ab initio programs; 2010; see <http://www.molpro.net/>.

(52) Simons, G.; Parr, R.; Finlan, J. New alternative to Dunham potentials for diatomic-molecules. *J. Chem. Phys.* **1973**, *59*, 3229–3234.

(53) Kozin, I. N.; Law, M. M.; Tennyson, J.; Hutson, J. M. Calculating energy levels of isomerizing tetraatomic molecules: II. The vibrational states of acetylene and vinylidene. *J. Chem. Phys.* **2005**, *122*, 064309.

(54) Light, J. C.; Carrington, T., Jr. Discrete-variable representations and their utilization. *Adv. Phys. Chem.* **2000**, *114*, 263–310.

(55) Tennyson, J.; Sutcliffe, B. T. The ab initio calculation of the vibration–rotation spectrum of triatomic systems in the close-coupling approach with KCN and H₂Ne as examples. *J. Chem. Phys.* **1982**, *77*, 4061–4072.

(56) Urru, A.; Kozin, I. N.; Mulas, G.; Braams, B. J.; Tennyson, J. Rovibrational spectra of C₂H₂ based on variational nuclear motion calculations. *Mol. Phys.* **2010**, *108*, 1973–1990.

(57) Jensen, P.; Bunker, P. R. *Molecular Symmetry and Spectroscopy*; NRC Research Press: Ottawa, Ontario, Canada, 1998.

(58) Hougen, J. T. Summary of group theoretical results for microwave and infrared studies of H₂O₂. *Can. J. Phys.* **1984**, *62*, 1392–1402.

(59) Cooley, J. W. *Math. Comp.* **1961**, *15*, 363–374.

(60) Numerov, B. *Mon. Not. R. Astron. Soc.* **1924**, *84*, 592–602.

(61) Polyansky, O. L.; Zobov, N. F.; Viti, S.; Tennyson, J.; Bernath, P. F.; Wallace, L. K band spectrum of water in sunspots. *Astrophys. J.* **1997**, *489*, L205–L208.

(62) Tinetti, G.; Vidal-Madjar, A.; Liang, M.-C.; Beaulieu, J.-P.; Yung, Y.; Carey, S.; Barber, R. J.; Tennyson, J.; Ribas, I.; Allard, N.; et al. Water vapour in the atmosphere of a transiting extrasolar planet. *Nature* **2007**, *448*, 169–171.

(63) Tennyson, J.; Yurchenko, S. N. ExoMol: molecular line lists for exoplanet and other atmospheres. *Mon. Not. R. Astron. Soc.* **2012**, *425*, 21–33.

(64) Warmbier, R.; Schneider, R.; Sharma, A. R.; Braams, B. J.; Bowman, J. M.; Hauschildt, P. H. Ab initio modeling of molecular IR spectra of astrophysical interest: application to CH₄. *Astron. Astrophys.* **2009**, *495*, 655–661.

(65) Carter, S.; Sharma, A. R.; Bowman, J. M. First-principles calculations of rovibrational energies, dipole transition intensities and partition function for ethylene using MULTIMODE. *J. Chem. Phys.* **2012**, *137*, 154301.

(66) Carter, S.; Handy, N. C. RVIB4: A tetraatomic rovibrational variational code; 2007.

(67) Flaud, J.-M.; Camy-Peyret, C.; Johns, J. W. C.; Carli, B. The far infrared spectrum of H_2O_2 . First observation of the staggering of the levels and determination of the cis barrier. *J. Chem. Phys.* **1989**, *91*, 1504–1510.

(68) Perrin, A.; Valentin, A.; Flaud, J. M.; Camy-Peyret, C.; Schriver, L.; Schriver, A.; Arcas, P. The $7.9\text{-}\mu\text{m}$ band of hydrogen peroxide – line positions and intensities. *J. Mol. Spectrosc.* **1995**, *171*, 358–373.